Rail corrugation growth on small radius curves

Peter T. Torstensson
CHARMEC / Department of Applied Mechanics
Chalmers University of Technology, Göteborg, Sweden

17th Nordic Seminar on Railway Technology,
Tammsviks herrgård, Bro, October 3-4, 2012

Contents

Rutting corrugation at SL

Corrugation characteristics

[P.T. Torstensson, J.C.O. Nielsen, Wear, 2009]

- Curve radius 120 m and vehicle speed about 30 km/h
- Corrugation wavelengths 5 cm and 8 cm
- Within a grinding interval of one year, corrugation with maximum peak-to-peak magnitude 0.15 mm develops on the low rail
- Roughness growth was observed until the measurement 300 days after grinding. Thereafter only limited additional growth was generated

Corrugation remedy

[New measurement campaign, intended for international publication]

- Application of a friction modifier prevents the re-development of corrugation after rail grinding

Roughness level in 1/3 octave bands, friction modifier applied

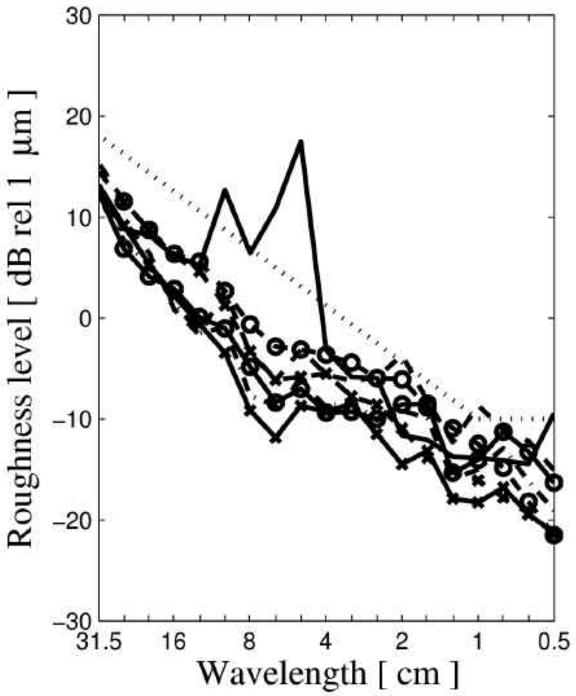

Laboratory investigation

Rail irregularity measured with a coordinate measurement machine

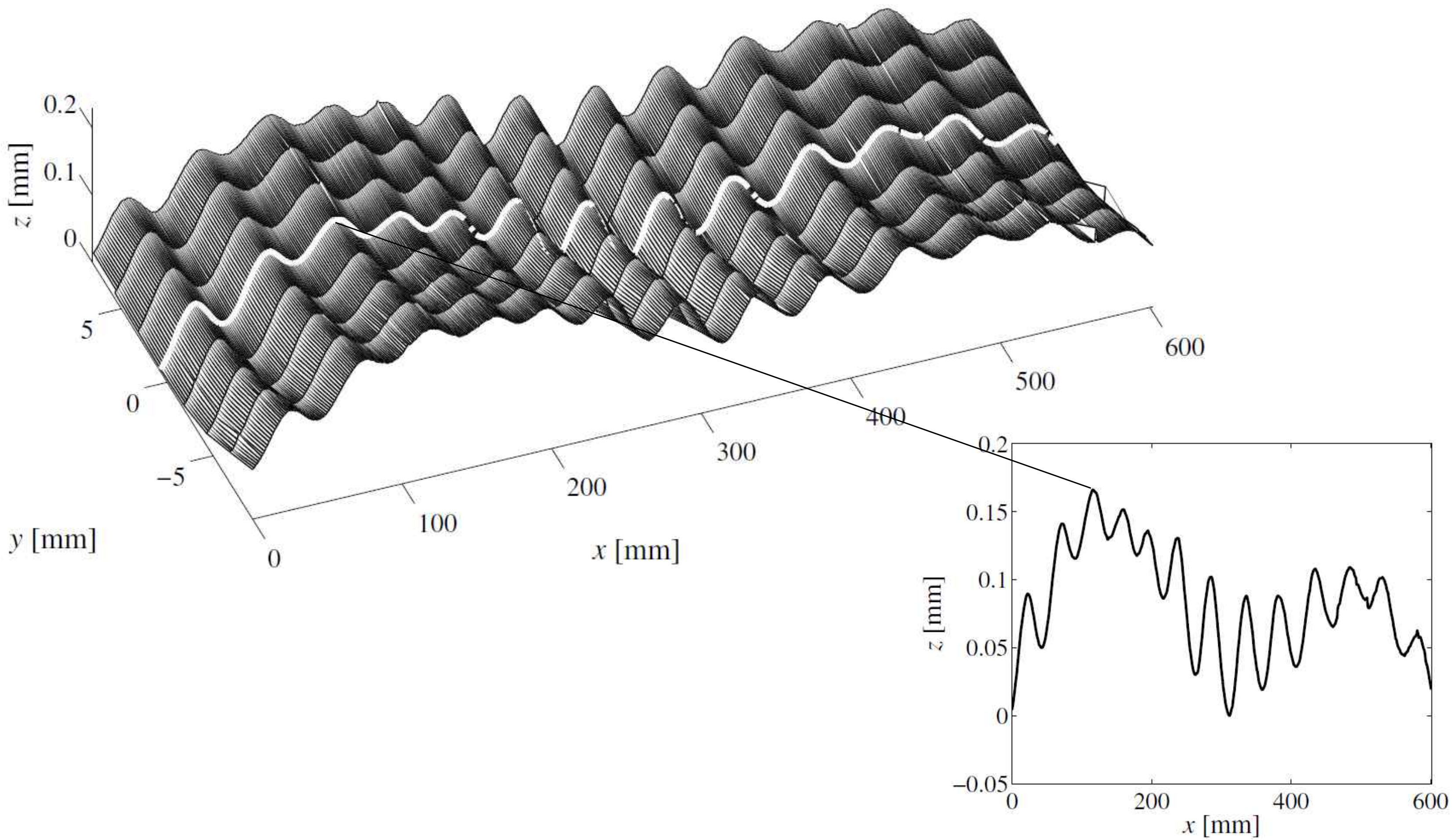

Laboratory investigation

Cross-section, longitudinal cut

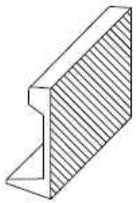

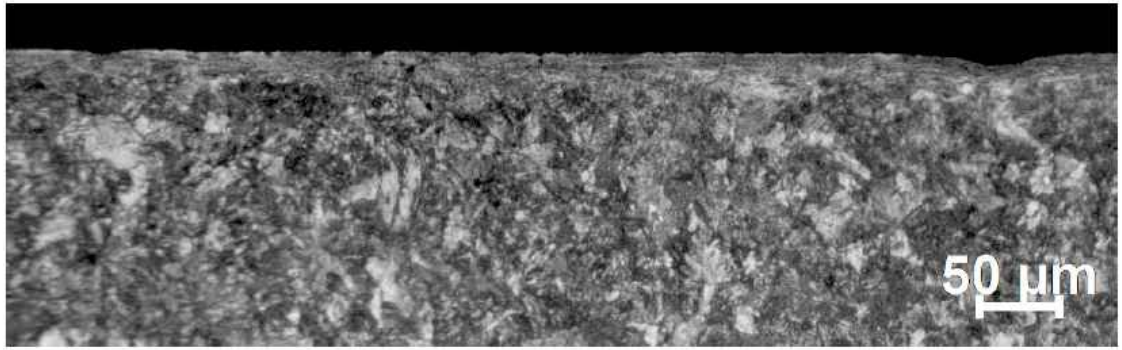

Cross-section, lateral cut

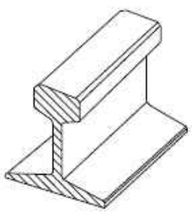

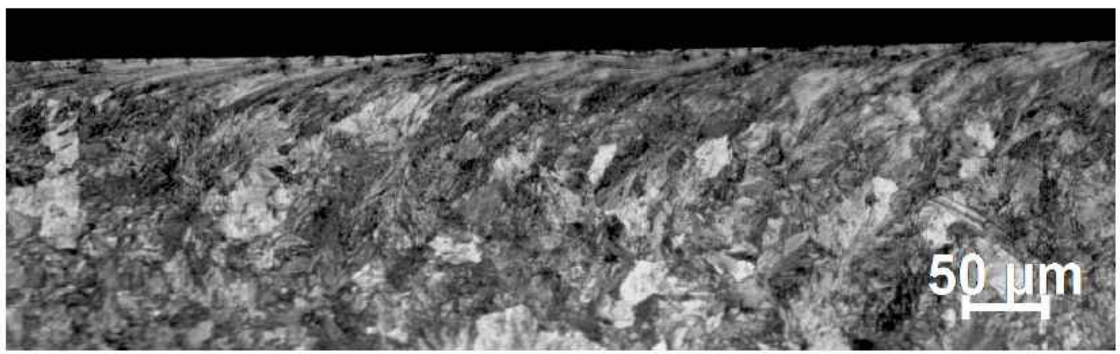

- *Lateral plastic flow down to a depth of 45 µm orientated towards the field side*
- *No difference in microstructure at corrugation crests and troughs was observed*

Modelling

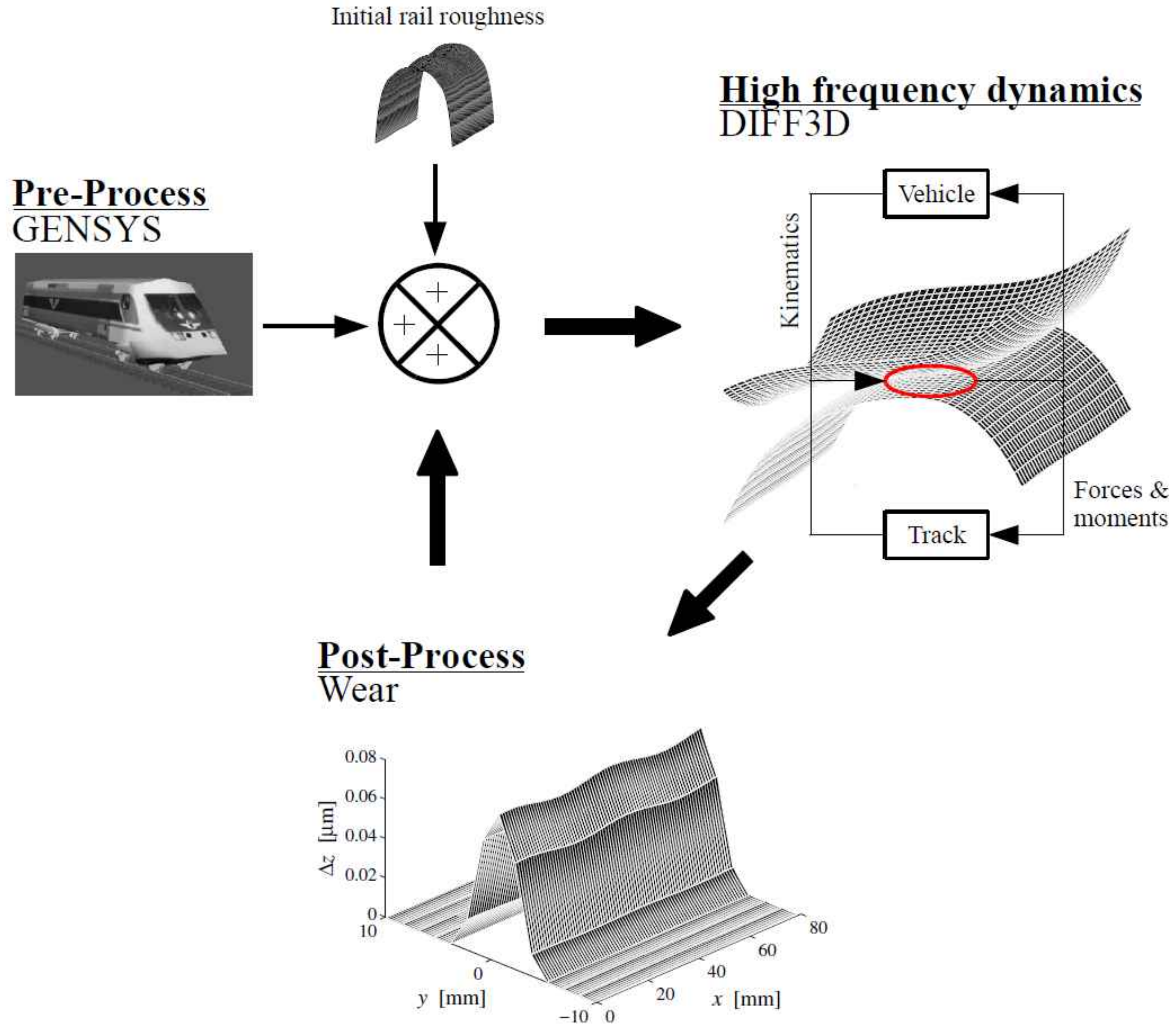
Initial rail roughness
High frequency dynamics
DIFF3D
Pre-Process
GENSYS
Vehicle
Kinematics
Forces &
moments
Track
Post-Process
Wear
0.08
0.06
0.04
0.02
0
Δz [μm]
10
0
−10
y [mm]
0
20
40
60
80
x [mm]

Non-Hertzian/non-steady contact model

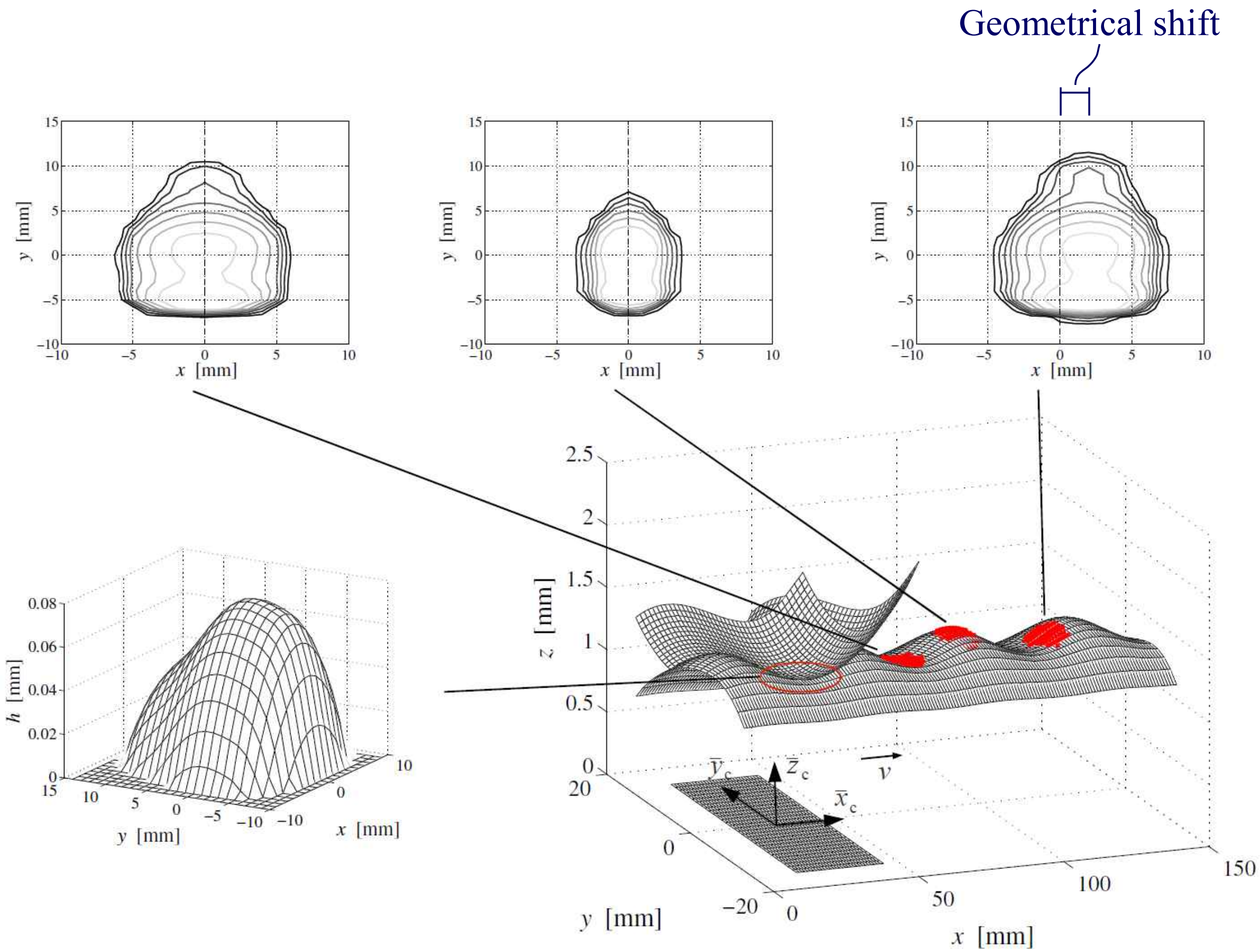

[Illustration of a wheel rolling on a 4 cm single wavelength irregularity]

Curving behaviour of a C20 metro train

Curving diagram for bogie 21 in a C20 metro train. R = 125 m, v = 32.5 km/h

Friction coefficient 0.6

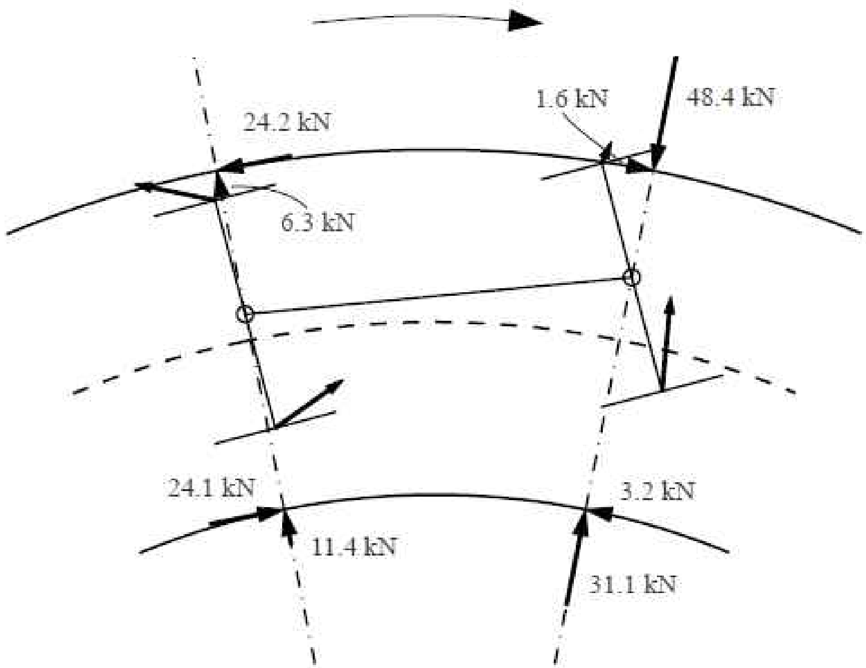

- *The large angle of attack (AOA) of the leading wheelset generates large magnitude lateral creep forces*
- *The trailing wheelset obtains a close to radial steering position but the deficient rolling radius difference creates large magnitude longitudinal creep forces*

Curving behaviour of a C20 metro train

Curving diagram for bogie 21 in a C20 metro train. *R* = 125 m, *v* = 32.5 km/h

Friction coefficient 0.3

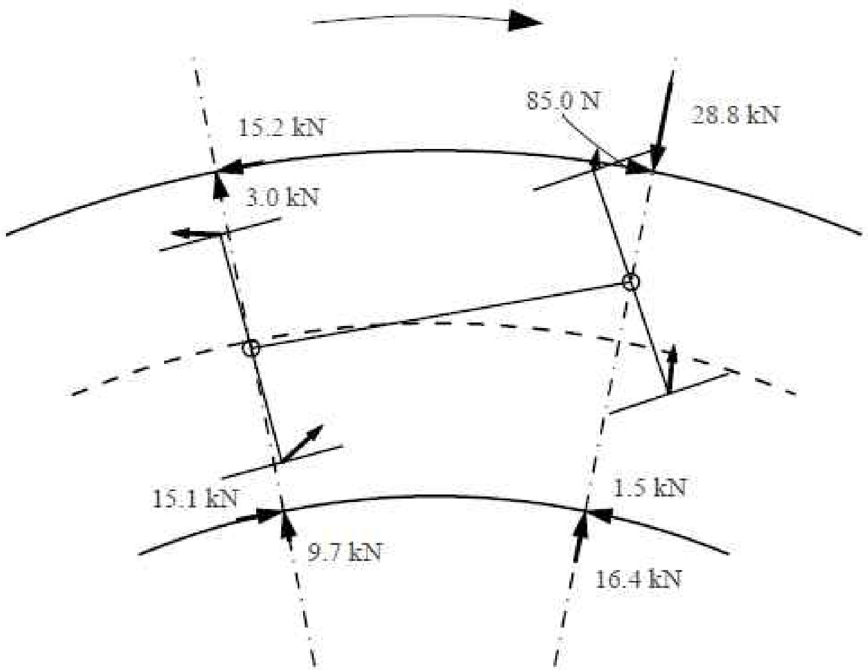

- *Full sliding in all wheel–rail contacts*
- *Compared to friction coefficient 0.6, the reduced steering moment results in an increased AOA of the leading wheelset and a displacement of the trailing wheelset towards the low rail*

Long-term roughness growth

Quotient between the initial and predicted irregularity after 400 wheel passages calculated for the low rail contact of the leading wheelset

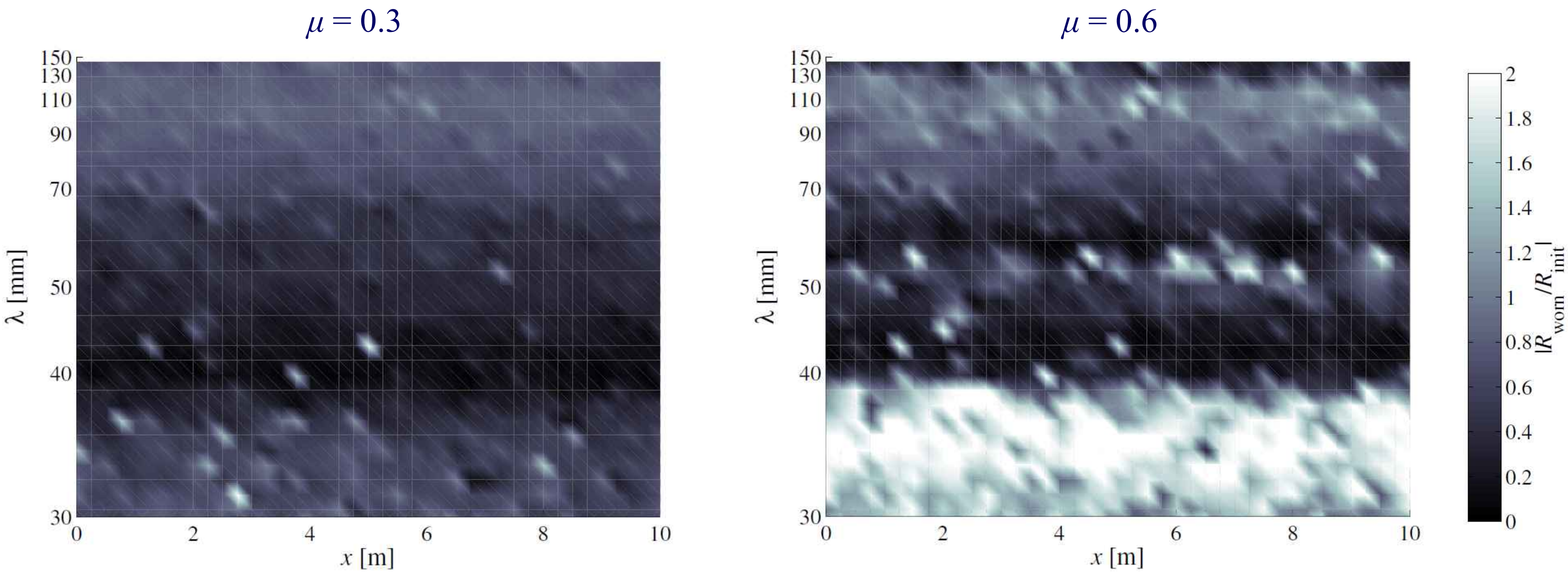

- *No growth of roughness is predicted for friction coefficient 0.3 (e.g. friction modifier)*
- *For friction coefficient 0.6 growth of roughness is predicted at several wavelengths*

[Results calculated for the non-Hertzian/non-steady contact model. Broadband wavelength rail irregularity modelled with magnitude according to the limit in ISO3095. Curve radius 120 m and vehicle speed 25 km/h]

Long-term roughness growth

Development of a single wavelength initial irregularity of wavelength 3.8 cm

Corrugation formation

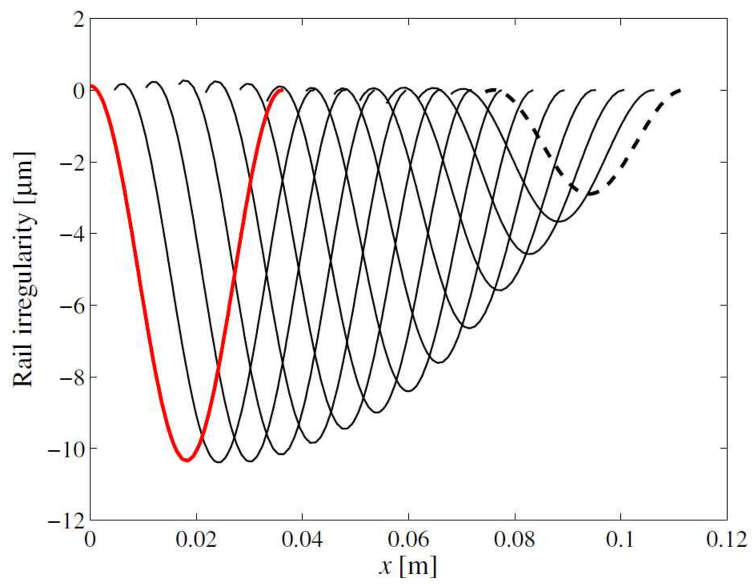

Phase

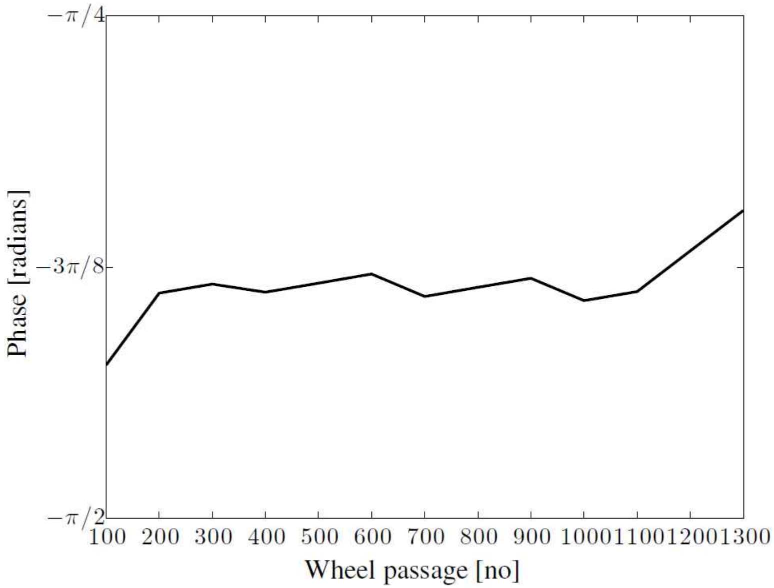

Roughness growth stops due to a decreasing phase between the calculated wear depth and the initial rail irregularity

[Accumulated wear calculated for the non-Hertzian/non-steady contact model for after 1200 wheel passages. Initial single wavelength rail irregularity of 3.8 cm wavelength modelled with magnitude according to the limit in ISO3095. Friction coefficient 0.6, curve radius 120 m and vehicle speed 25 km/h]

Wheel–rail contact generating corrugation

Magnitude (1/24 octave bands) of the transfer function $\overline{H}$ calculated for the low rail contact of the leading and trailing wheelsets

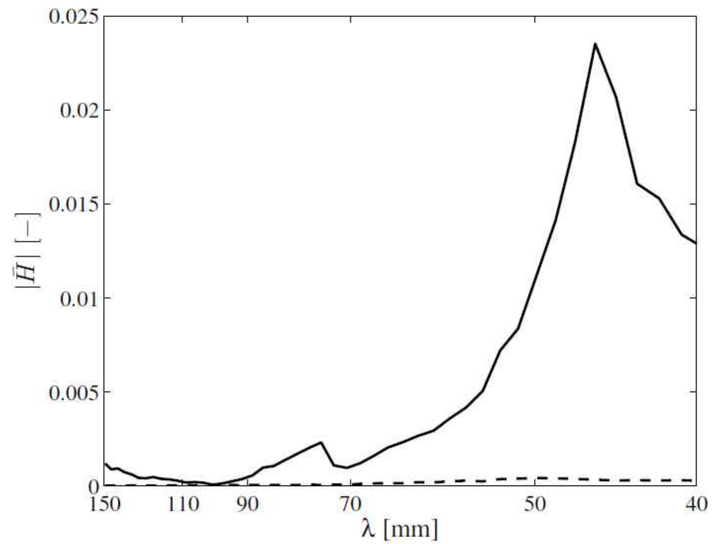

—: low rail contact of leading wheelset, – – : low rail contact of trailing wheelset

Growth of corrugation on the curve between Alvik and Stora mossen is generated by the low rail contact of the leading wheelset in passing bogies

[Accumulated wear after one wheel passage calculated for the Hertz/FASTSIM contact model. Broadband initial rail roughness modelled with magnitude according to the limit in ISO3095. Curve radius 120 m, friction coefficient 0.6 and vehicle speed 30 km/h]

Wavelength-fixing mechanism

Wavelength-fixing mechanism associated with the roughness peak at about 5 cm

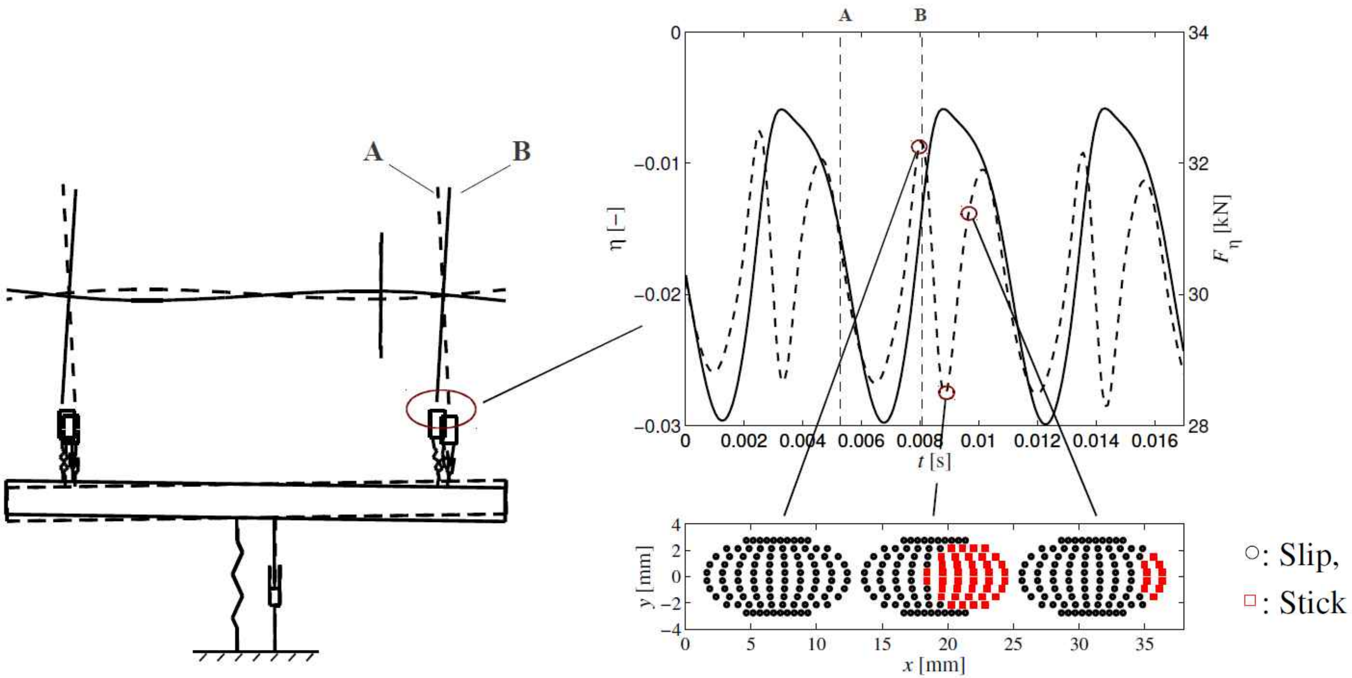

Wavelength-fixing mechanism primarily associated with the first antisymmetric bending eigenmode of the wheelset

[A single wavelength irregularity of wavelength 4.5 cm and amplitude 32 μm is modelled on the low rail. Friction coefficient 0.6, curve radius 120 m and vehicle speed 30 km/h]

Wavelength-fixing mechanism

Wavelength-fixing mechanism associated with the roughness peak at about 8 cm

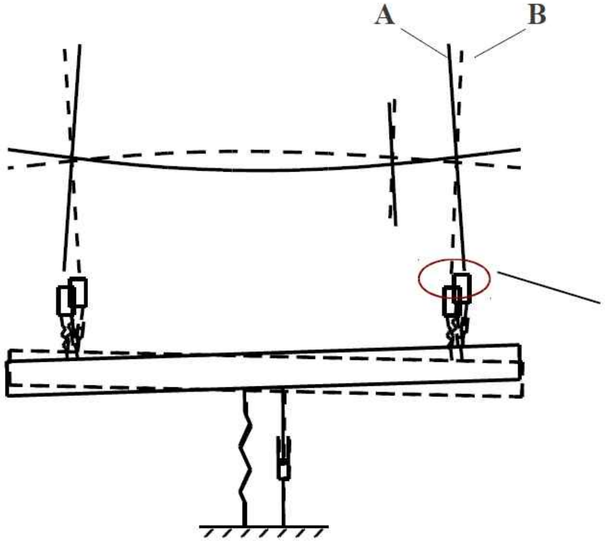

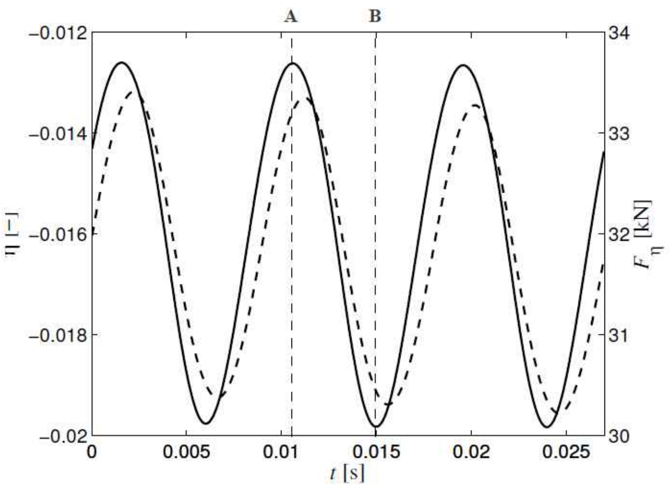

Wavelength-fixing mechanism primarily associated with the first symmetric bending eigenmode of the wheelset

[A single wavelength irregularity of wavelength 7.5 cm and amplitude 32 μm is modelled on the low rail. Friction coefficient 0.6, curve radius 120 m and vehicle speed 30 km/h]

Long-term roughness development

Predicted development of roughness on the low rail

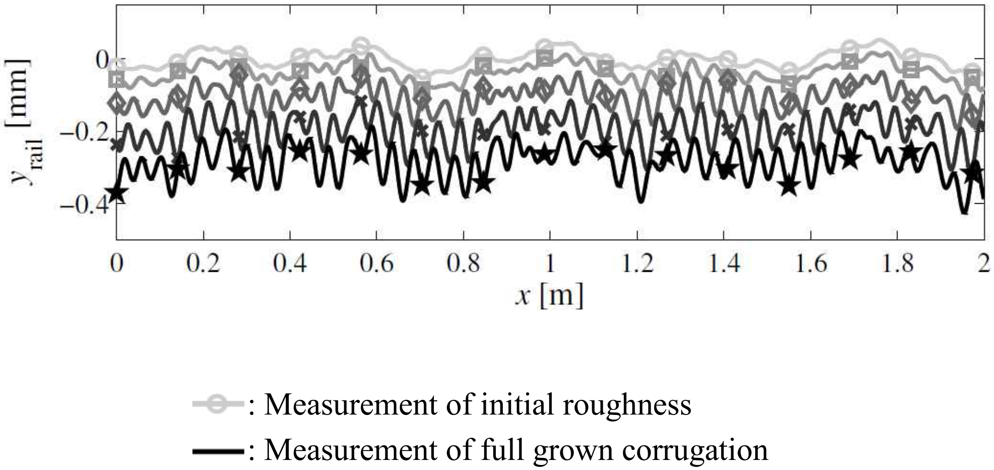

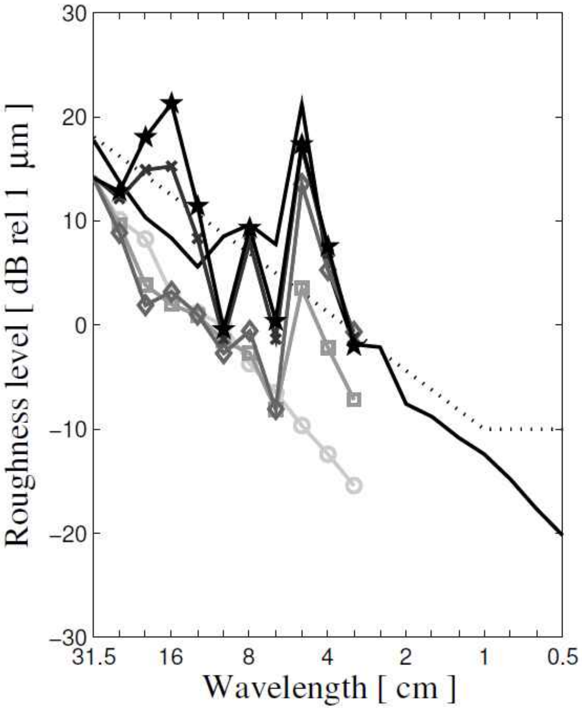

[Development of rail roughness for 40 000 wheel passages calculated for the non-Hertzian and non-steady contact model. Broadband initial rail roughness modelled with magnitude according to the limit in ISO3095. Curve radius 120 m, friction coefficient 0.6, vehicle speed 30 km/h and 0.95 · D_w]

Conclusions and future work

Conclusions

- Corrugation growth on the curve between Alvik and Stora mossen is generated by the leading wheelset of passing boiges. The acting wavelength-fixing mechanisms are primarily influenced by the first symmetric and first antisymmetric bending eigenmodes of this wheelset
- For friction coefficient 0.3, predictions of corrugation growth on the low rail of a 120 m radius curve showed decreasing roughness magnitudes in the entire studied wavelength interval. For friction coefficient 0.6, corrugation developed at several wavelengths. This agrees with observations from a measurement campaign that shows friction modification is a successful mitigation measure to prevent the re-development of corrugation
- For a single wavelength and broadband roughness initial rail irregularity, the rapid initial growth of corrugation was predicted to eventually stop. The fully grown corrugation moved backwards (with respect to the rolling direction of the train) with a constant amplitude

Suggestions for future work

- Verify the predicted longitudinal translation of the fully grown corrugation in a measurement campaign
- Investigate important parameters that determine the growth of corrugation, e.g. magnitude of contact forces, amplitude and wavelength content of initial roughness

Thank you for your attention!

Long-term roughness growth

Development of a single wavelength initial irregularity of wavelength 5 cm

$\mu = 0.3$

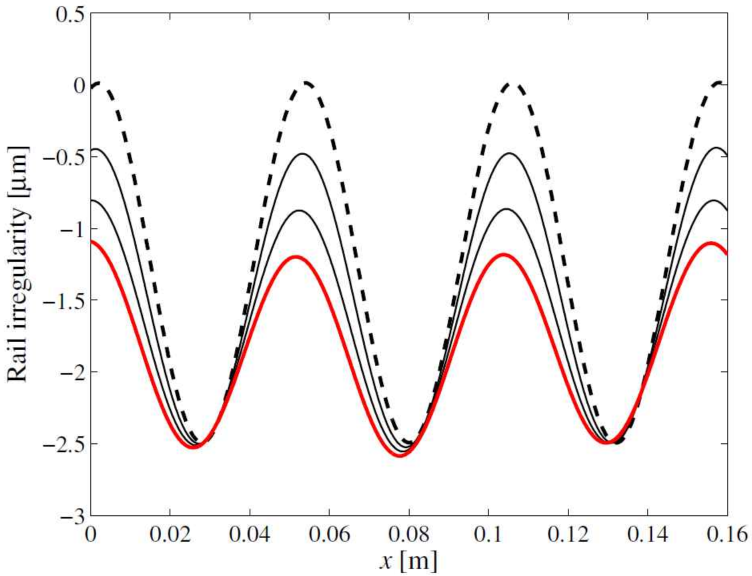

$\mu = 0.6$

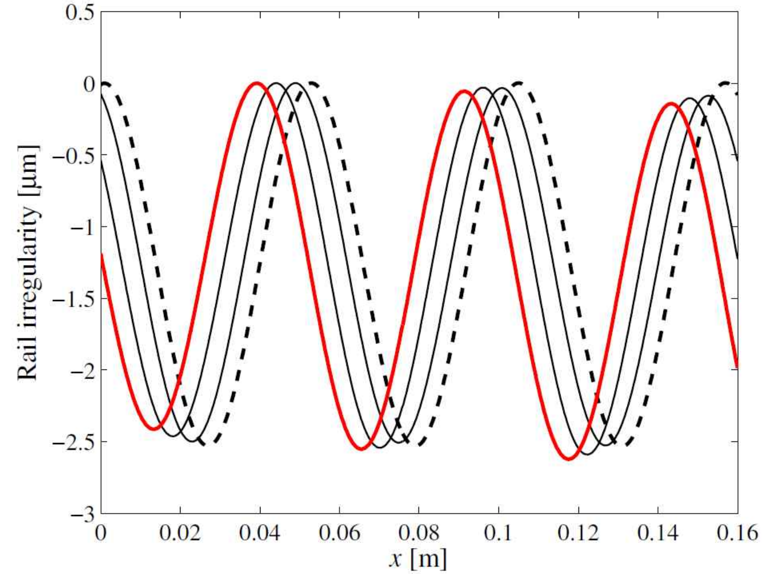

- *For friction coefficient 0.3 the corrugation wears off for increasing number of wheel passages*
- *For friction coefficient 0.6 the corrugation moves backwards with constant amplitude*

[Accumulated wear calculated for the non-Hertzian/non-steady contact model after 300 wheel passages. Initial single wavelength rail irregularity of 5 cm wavelength modelled with magnitude according to the limit in ISO3095. Curve radius 120 m and vehicle speed 25 km/h]

Purpose

- Present a model for simulation of long-term rail roughness growth on small radius curves
- Investigate the influence of non-Hertzian and non-steady contact effects on calculations of long-term roughness growth
- Investigate the development of corrugation on the small radius curve on the Stockholm metro selected for the measurement campaign

Prediction of corrugation growth..

..according to tradition

Initial non-corrugated rail surface

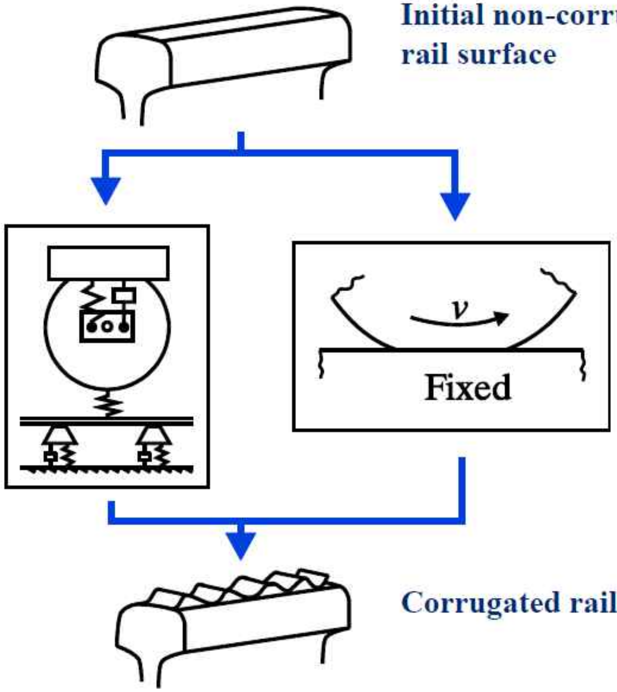

Wavelength-fixing mechanism
- Track and wheelset resonances
- Stick-slip action

Damage mechanism
- Wear
- Plastic flow

Corrugated rail surface

Modelling

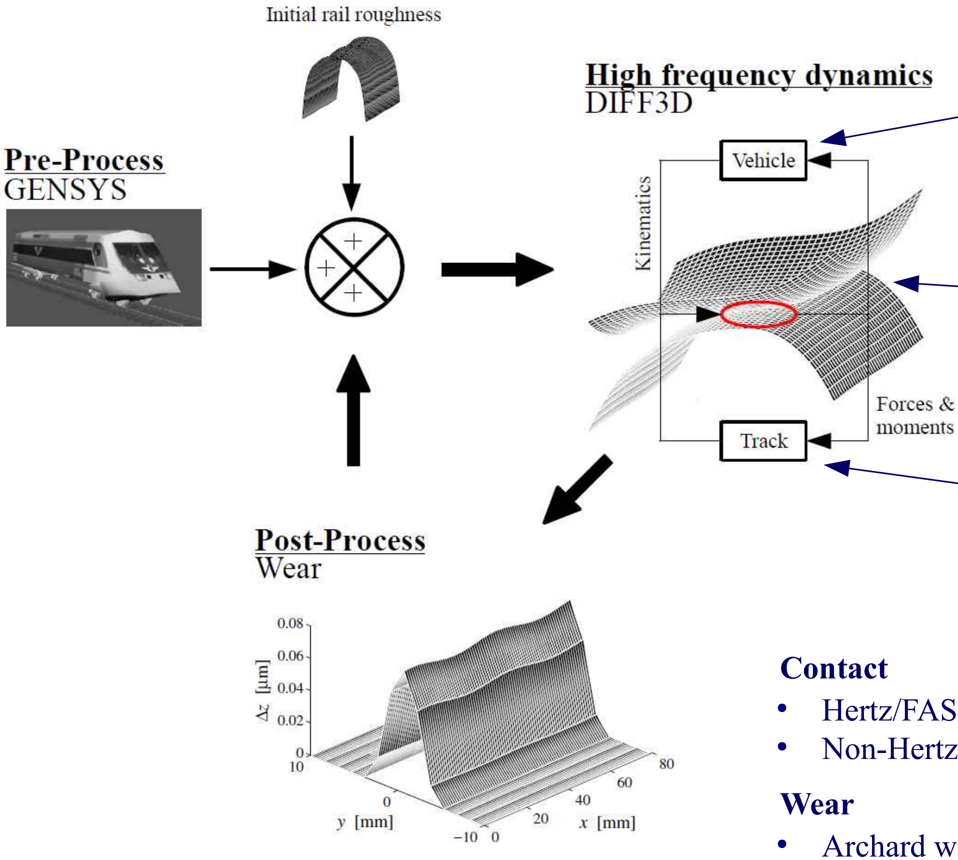

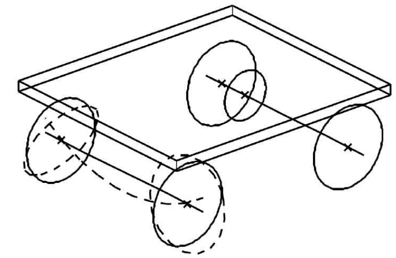

- Accurate contact detection algorithm
- Hertz/FASTSIM

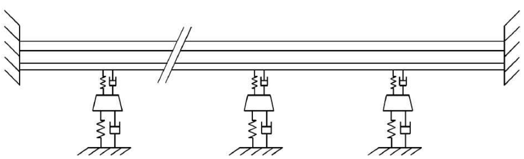

Contact

- Hertz/FASTSIM
- Non-Hertzian/non-steady

Wear

- Archard wear law

Modelling

Archard wear law applied on one sliding contact element

$$\Delta z = k_w \frac{p_z \Delta d}{H}$$

$$\Delta d = |v_s| \Delta t$$

$$\Delta t = \Delta x / v$$

Δz – wear depth [m]
k_w – wear coefficient [-]
p_z – normal contact pressure [N/m^2]
H – hardness [N/m^2]
v_s – slip velocity [m/s]

Mapping of wear depth Δz onto the rail surface

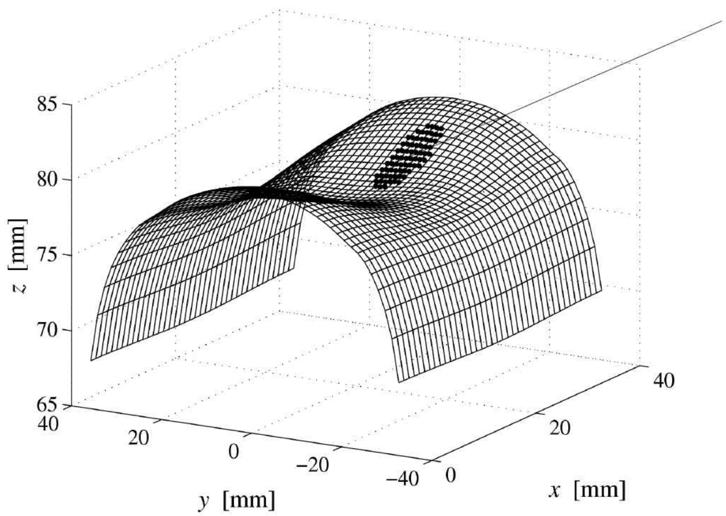

Mapping of accumulated wear of contact element c_n (hatched) onto the rail mesh

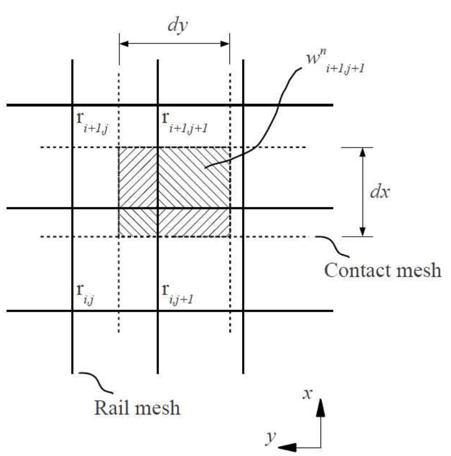

Measured rail roughness

Roughness level in 1/3 octave bands. Friction modification applied on the southbound track

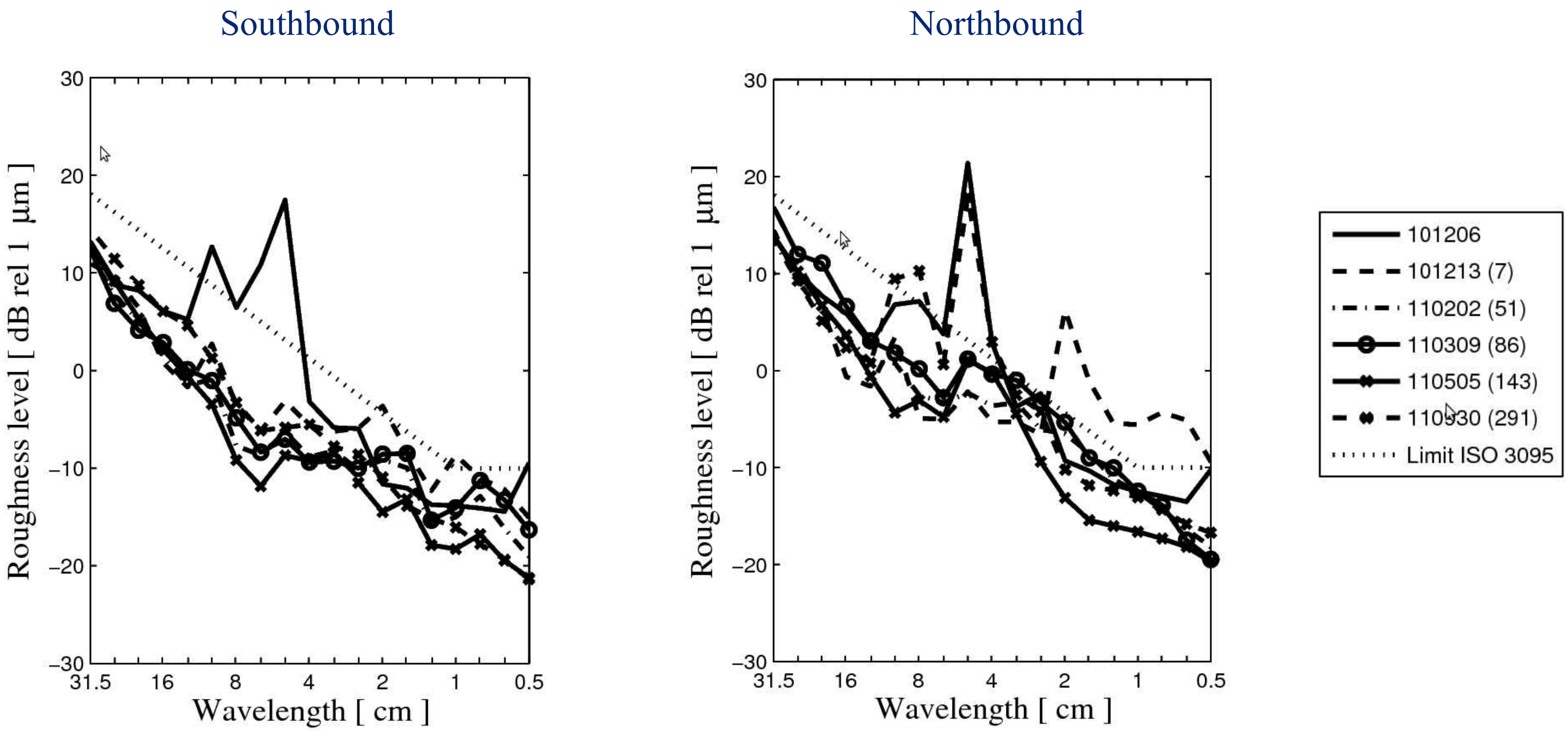

No growth of roughness is observed when friction modification is applied

Measured rail acceleration

Acceleration level spectra

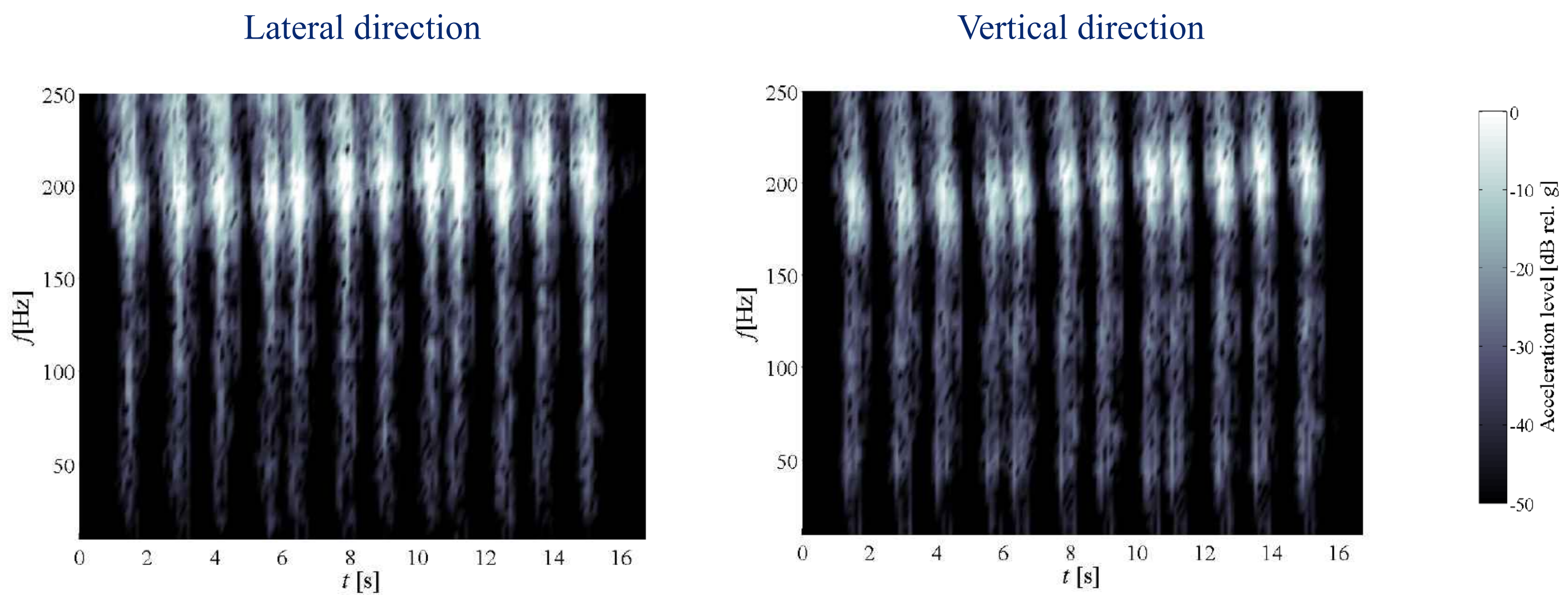

- *Acceleration levels measured in lateral direction exceeds those obtained in vertical direction*
- *Increased acceleration level observed at approximately 190 Hz is caused by corrugation wavelength 5 cm (vehicle speed approximately 35 km/h)*

Transfer function $\overline{H}(1/\lambda)$

Magnitude and phase of the transfer function, $\overline{H}(1/\lambda)$, between the calculated wear depth and the rail irregularity:

Magnitude: $|\overline{H}(1/\lambda)| = \dfrac{A_{\Delta Z}}{A_R}$

Phase: $\arg(\overline{H}(1/\lambda)) = \alpha$

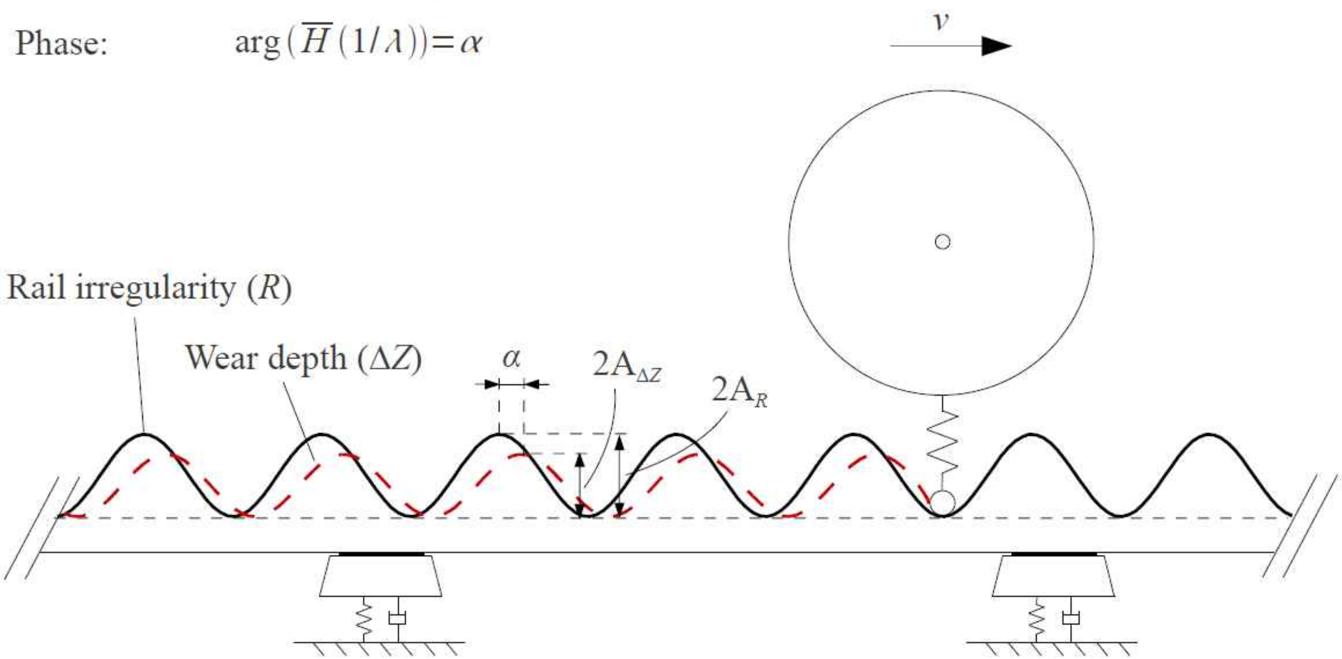

Long-term roughness growth, high rail

(a) Phase of the transfer function $\overline{H}$ calculated for different contact locations and friction coefficients
(b) Quotient between the initial and calculated irregularity after 400 wheel passages for μ = 0.6

(a)

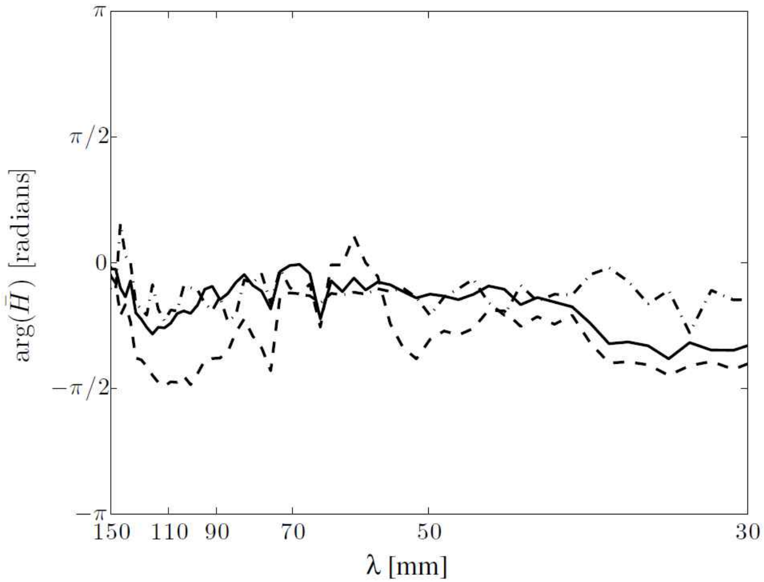

(a)

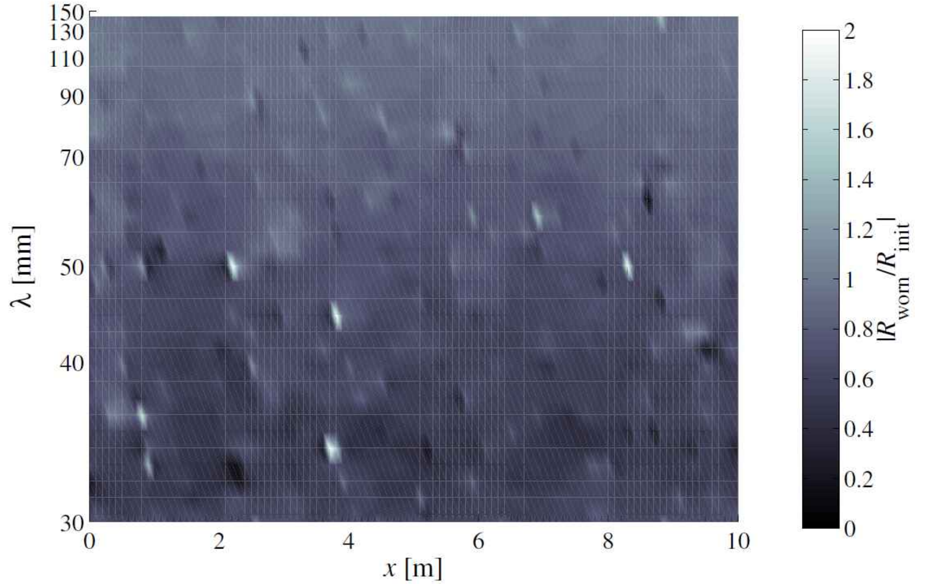

—: Low rail contact, μ = 0.3, - - : Low rail contact, μ = 0.6, -·-: High rail contact, μ = 0.6

No roughness growth is predicted for the high rail contact of the trailing wheelset

[Broadband wavelength rail irregularity modelled with magnitude according to the limit in ISO3095. Curve radius 120 m and vehicle speed 25 km/h]

Long-term roughness growth, high rail

(a) Phase of the transfer function $\overline{H}$ calculated for different contact locations and friction coefficients

(b) Quotient between the initial and calculated irregularity after 400 wheel passages for μ = 0.6

(a)

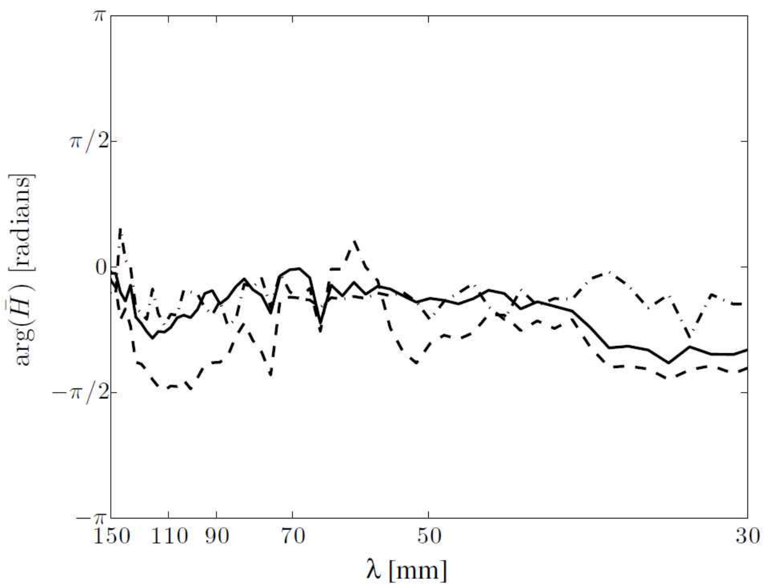

(a)

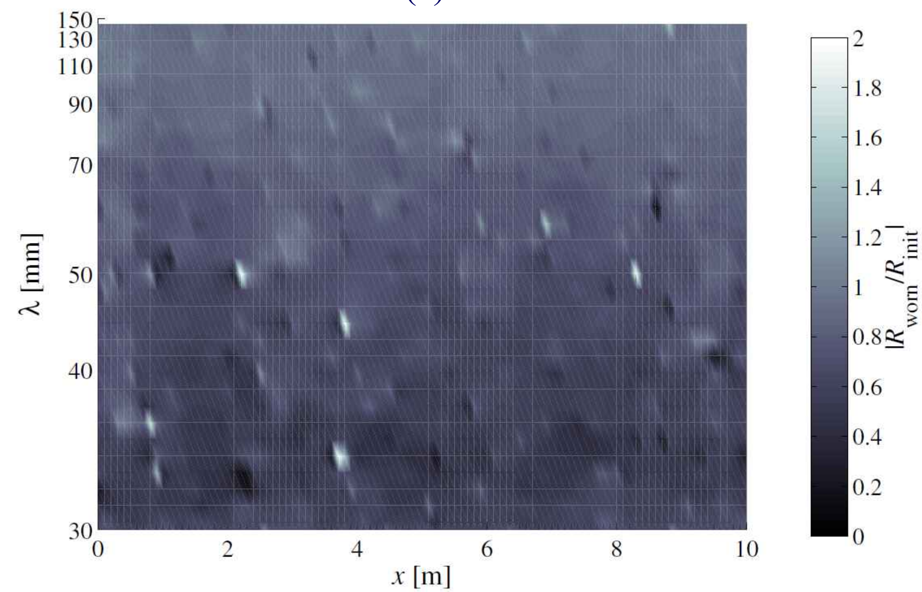

—: Low rail contact, μ = 0.3, - - : Low rail contact, μ = 0.6, -·-: High rail contact, μ = 0.6

➡ *No roughness growth is predicted for the high rail contact of the trailing wheelset*

[Broadband wavelength rail irregularity modelled with magnitude according to the limit in ISO3095. Curve radius 120 m and vehicle speed 25 km/h]

Corrugation development